Plant Soil
https://doi.org/10.1007/s11104-024-07128-1

RESEARCH ARTICLE

Shift of the ecosystem nitrogen cycle from open to closed within a century along a glacial retreat chronosequence at Mount Gongga, southwest China

Nuria Basdediós · Samuel Hardegger · Adrien Mestrot · Jipeng Wang · Jun Zhou · Haijian Bing · Yanhong Wu · Wolfgang Wilcke

Received: 21 August 2024 / Accepted: 29 November 2024

Abstract

Aims To improve our understanding of N cycle development during primary succession after glacial retreat, we (i) assessed the role of biological N_2 fixation, (ii) determined gross ammonification rates to identify the onset of mineralization, (iii) quantified the retention of $^{15}NH_4^+$ and $^{15}NO_3^-$ in various ecosystem compartments to evaluate the accumulation of deposited N and (iv) followed the $^{15}NH_4^+$ label into the soil NO_3^- pool to explore the development of nitrification along the subtropical alpine Hailuogou glacial retreat chronosequence, SW China.

Methods We measured N stocks and $\delta^{15}N$ values in the dominant tree species, organic layer and 0–10 cm of the mineral soil and quantified N turnover rates and accumulation via ^{15}N tracer experiments.

Results N accumulated in the ecosystem at a fast mean rate of 4.5 ± 1.0 g m^{-2} yr^{-1} favored by an initially near-neutral soil pH value. The $\delta^{15}N$ values of the vegetation started near 0‰ and decreased to a range of -2.7 to -4.4‰ in 127 years. Gross ammonification rates were initially low but increased with ecosystem age from 0.025 to 50.6 mg kg^{-1} d^{-1} N, matching those of mature (sub)tropical forests. The maximum accumulation of deposited N shifted from the bryophyte via the shrub layer to the soil organic layer. The $^{15}NH_4^+$ label hardly appeared in the NO_3^- pool reflecting little nitrification.

Conclusions Strong initial biological N_2 fixation and retention of deposited N was succeeded by a tight N cycling between soil and vegetation at the older sites within approximately 120 yr.

Keywords Biological N_2 fixation · Glacial retreat chronosequence · Gross mineralization · Natural isotope abundance · Primary succession · Pulse-chase experiment

Responsible Editor: Benjamin L. Turner.

Supplementary Information The online version contains supplementary material available at https://doi.org/10.1007/s11104-024-07128-1.

N. Basdediós (✉) · W. Wilcke
Karlsruhe Institute of Technology (KIT),Institute of Geography and Geoecology, Reinhard-Baumeister-Platz 1, 76131 Karlsruhe, Germany
e-mail: nuria.basdedios@kit.edu

S. Hardegger · A. Mestrot
Institute of Geography, University of Bern, Hallerstr. 12, 3012 Bern, Switzerland

J. Wang · J. Zhou · H. Bing · Y. Wu
Key Laboratory of Mountain Surface Processes and Ecological Regulation, Institute of Mountain Hazards and Environment, Chinese Academy of Sciences, Chengdu 610299, China

Introduction

Mountain glaciers are globally retreating since the second half of the nineteenth century (IPCC 2023),

Published online: 09 January 2025

leaving freshly deposited rock debris behind, on which new ecosystems develop (Delgado-Baquerizo et al. 2020; Ficetola et al. 2024; Hugonnet et al. 2021). If the debris does not include fossil organic matter, it is free of N, the quantitatively most needed plant nutrient (Vitousek & Howarth 1991; LeBauer & Treseder 2008). In the absence of plants in the early stages of primary succession, N supply originates from atmospheric deposition and free-living (non-symbiotic) N_2-fixing bacteria and archaea (Göransson et al. 2016; Reed et al. 2011). Once N-containing organic compounds are incorporated into the soil as organic matter (SOM), mineralization releases plant-available N (NH_4^+ and NO_3^-) into the soil solution (Blevins 1989). The advancing ecosystem succession increases above- and belowground litter. The litter accumulates if it is not decomposed within one year after its deposition, which commonly occurs in humid and cool climates like those in glacier forefields (Hodkinson et al. 2003; Wietrzyk et al. 2018; Vogt et al. 1983). As a consequence, an organic layer on top of the mineral soil is formed, which serves as a nutrient reservoir from which N is increasingly mineralized (Cleveland et al. 2013; Khedim et al. 2021; Lilienfein et al. 2001). The advancing vegetation succession increasingly retains mineral N because of larger N uptake and reduced seepage fluxes resulting from increased evapotranspiration (Feng et al. 2016). The associated establishment of a microbial community further increases N retention through immobilization (Jiang et al. 2019). Altogether, this contributes to the establishment of a closed N cycle that ensures plant nutrition over longer time scales (Perakis and Hedin 2001; Yan et al. 2024).

The natural abundance of stable N isotopes (^{15}N values) in soils and plants offers a powerful tool for evaluating N dynamics in ecosystems. The N that reaches the soil by biological N fixation shows a $\delta^{15}N$ value near that of the atmospheric N_2, which is by definition 0‰. As a consequence, the $\delta^{15}N$ values of soils and plants can be used to quantify the proportion of atmospheric N_2 used by legumes and actinorhizal trees (Boddey et al. 2000; Craine et al. 2015; Shearer and Kohl 1986). Soil processes, such as N mineralization, nitrification, and denitrification, typically involve incomplete chemical reactions that selectively discriminate against ^{15}N causing kinetic isotope fractionation (Mariotti et al. 1981; Blackmer and Bremmer 1977). Consequently, $\delta^{15}N$ values can reflect the openness of the N cycle within an ecosystem, with higher values indicating greater losses through processes like denitrification and leaching, which favor the loss of ^{14}N as N_2O, N_2 or NO_3^-, thereby enriching the remaining soil N pool in ^{15}N (Austin & Vitousek 1998; Högberg 1990; Vitousek 2002). The distinct $\delta^{15}N$ signatures of the different soil N pools are then reflected in the $\delta^{15}N$ values of plants that rely on these pools (Amundson et al. 2003; Högberg 1997; Houlton et al. 2007; Robinson 2001).

In addition to the natural abundance of N isotopes, experiments with ^{15}N labeling provide valuable insights into the N cycling dynamics within ecosystems. A common approach to determine N transformation rates in soils are ^{15}N-pool-dilution experiments, where a well-defined soil volume is labeled with highly ^{15}N-enriched N and the dilution rate of the enriched pool by newly formed N species is monitored (Davidson et al. 1991; Hart et al. 1994). The retention of deposited N in ecosystems can be determined with pulse-chase experiments, during which an isotope label is introduced and tracked across all major ecosystem compartments over a specific period of time (Hart et al. 1994; Lehmann et al. 2004). Labeling the soil with $^{15}NH_4^+$ or $^{15}NO_3^-$ allows for tracing the fate of the different N species through the ecosystem (Braun et al. 2018). Some previous studies reported a higher recovery of $^{15}NH_4^+$ than $^{15}NO_3^-$ tracer in the upper mineral soil, primarily attributed to greater NO_3^- leaching into deeper soil layers (e.g., Buchmann et al. 1996; Groffman et al. 1996). However, Perakis and Hedin (2001) reported a similar long-term retention of both $^{15}NH_4^+$ and $^{15}NO_3^-$ in a forest in southern Chile, and Providoli et al. (2006) even found a stronger retention of $^{15}NO_3^-$ than of $^{15}NH_4^+$ in a coniferous mountain forest in Switzerland, indicating that the interplay between amended N forms and soil processes is strongly context-dependent. Additionally, by determining the recovery of $^{15}NH_4^+$ in the NO_3^- pool of the soil within the framework of the NH_4^+ pulse-chase experiment, we can assess nitrification—an approach that, to the best of our knowledge, has not been previously attempted.

The Hailuogou glacier in SW China has been continuously retreating since the late nineteenth century (Li et al. 2010), developing a soil and vegetation succession that had not been strongly disturbed by human activities at the time of our sampling between 2014

and 2017, rendering it an ideal area to study N cycling in the early stages of soil and vegetation development. Recent studies at the Hailuogou glacial retreat chronosequence have focused on N stoichiometry and its implication for nutrient limitation (Bing et al. 2016; Yang et al. 2014, 2021; Zhang et al. 2021), as well as its effects on the activity and diversity of soil microbial communities (Huang et al. 2023a; Li et al. 2020; Song et al. 2020). Despite the strong growth-limitation by N (Yang et al. 2021), the Hailuogou glacial retreat chronosequence shows a rapid vegetation succession starting with leguminous herbs and N_2-fixing shrub-microorganism symbioses, followed by half-mature broad-leaved tree forests, to a mixed forest dominated by conifers (Zhou et al. 2013) The oldest succession stage reaches the estimated mean biomass of mature temperate coniferous forests (307 Mg ha^{-1}, Cole and Rapp 1981) within 80 years (Luo et al. 2004). Because of the high energy cost, biological N_2 fixation largely disappears when the soil N availability increases above a threshold value (Vitousek & Howarth 1991; Zheng et al. 2019). In line with this, N_2-fixing plant–microbe symbioses such as *Hippophae tibetana* Schltdl. disappeared at the Hailuogou chronosequence after 40 years. Thereafter, the primary N resources originated from the mineralization of SOM, which progressively accumulates with increasing site age at a mean rate of 288 g m^{-2} $year^{-1}$ (Basdediós et al. 2022b). Basdediós et al. (2022b) suggested that the initial presence of carbonates in the glacial debris at a low concentration that buffered the soil pH around 7 facilitated the initial succession, because it provided near-optimum physico-chemical soil conditions for microbial activity including biological N_2 fixation. Deepening our knowledge of the processes regulating the N cycle including N fixation, mineralization, nitrification, and leaching and particularly their rates is crucial for understanding N dynamics in newly exposed ecosystems. This process understanding is particularly important in view of the mountain risks such as flooding and erosion originating from the globally increasing glacial retreat areas in response to climate change (Hock et al. 2019).

Hence, to investigate the role of N for the vegetation succession along the Hailuogou chronosequence, we (i) assessed the extent of biological N_2 fixation and the duration of the shift from predominant N_2 fixation to N mineralization with the help of ^{15}N values in bulk soils and in vegetation along the chronosequence, (ii) determined gross ammonification rates to pinpoint the onset of mineralization with a closed-system short-term ^{15}N labeling experiment, (iii) located and quantified the retention of deposited N in various ecosystem strata and (iv) followed the $^{15}NH_4^+$ label into the NO_3^- pool to determine the role of nitrification. We hypothesized that (i) N_2 fixation is particularly high in the early stage of the chronosequence because of favorable initial soil conditions, allowing for a fast shift to mineralization-driven N supply to the vegetation as reflected by an increasing N stock in the ecosystem, (ii) ammonification is quickly established and soon dominates the N supply of the vegetation, (iii) the main sink of the added ^{15}N shifts from initial moss-dominated organism communities via the vegetation to the soil, and (iv) there is little nitrification because of a rising plant N demand as biomass increases, which reduces the availability of NH_4^+ for nitrification.

Materials and methods

Study area

The Hailuogou glacier is located on the eastern slope of the Mount Gongga, in the transition zone of the Tibetan Plateau and the Sichuan Basin, southwest China (Fig. S1). Because of the worldwide increasing temperatures (IPCC 2023), the Hailuogou glacier has been retreating since the late nineteenth century (Li et al. 2010), developing a 2 km-long, 50–200 m-wide chronosequence, which spans an elevational range from 2800 to 2950 m above sea level (a.s.l.). Along the chronosequence, a primary vegetation succession has developed starting with leguminous herbs (i.e., *Astragalus adsurgens* Pall.) and N-fixing shrubs (i.e., *Hippophae tibetana* Schltdl.), followed by half- mature broad-leaved tree forests dominated by poplar (*Populus purdomii* Rehder), to a conifer-dominated mixed forest with Faber's fir [*Abies fabri* (Mast.) Craib] and Sargent spruce [*Picea brachytyla* (Franch.) E. Pritz (Table 1). The mean annual air temperature is 4.2 °C (Zhou et al. 2013). The mean annual precipitation is 1947 mm, with the majority of rainfall occurring between May and September (Wu et al. 2013).

The short time of pedogenesis (<130 years) resulted in soils without B horizons classified from youngest to

Table 1 Contributions of the dominating tree and bush species and mean chemical properties of the mineral topsoil soil along the Hailuogou Glacier retreat chronosequence, sampled in 2017, except for the 24 year old site which is from 2014

Site age [years]	Elevation [m a.s.l.]	Dominant species (relative abundance, canopy cover) [%]	pH (H_2O)	CO_3^{2-} [g kg^{-1}]	C_{org} [g kg^{-1}]	TN [g kg^{-1}]	C/N
0	2982	bare land	8.3 (0.0)	25 (1)	< 4.0	0.1 (0.1)	-
24	2947	*H. tibetana* (100%, canopy cover < 30%)	6.7 (0.2)	NA	NA	0.75 (0.1)	NA
37	2942	*H. tibetana* (100%, canopy cover 35%)	6.1 (0.1)	2 (1)	16.9 (2.7)	1.0 (0.1)	17 (0.2)
47	2922	*P. purdomii* (55–70%, canopy cover > 50%)	5.8 (0.2)	ND	14.1 (1.2)	1.2 (0.3)	12 (0.3)
59	2912	*A. fabri* (40–50%, canopy cover 40%) *P. purdomii* (40%, canopy cover 40%)	5.9 (0.1)	ND	10.8 (2.8)	0.8 (0.2)	14 (0.4)
87	2883	*A. fabri* and *P. brachytyla* (50–65%, canopy cover 60% and 20%, respectively)	4.9 (0.1)	< 0.5	28.9 (10.4)	1.9 (0.7)	15 (0.5)
127	2855	*P. brachytyla* and *A. fabri* (> 65%, canopy cover 60% and 40%, respectively)	5.2 (0.2)	< 0.5	47.7 (20.5)	3.4 (1.5)	14 (0.6)

The pH value of the 24 yr-old site was determined in 0.01 M $CaCl_2$ with a soil:solution ratio of 1:2.5 and converted to pH (H_2O) by adding 0.5. Only tree species with a trunk diameter ≥ 2.6 cm were included in calculating the relative abundance of each species (data adapted to our study sites from Li & Xiong 1995). The percent canopy cover was estimated visually for each individual tree on three replicate 20 m × 20 m plots by Luo et al. (2004) and adapted to our study sites (Basdediós et al 2022b). TN and C_{org} are total N and organic C concentrations, respectively. ND is not detected. NA is not available. Values in parentheses are standard errors ($n = 3$)

oldest as Leptic Calcaric to Folic Dystric Regosols (IUSS Working Group WRB 2022). With increasing time, the soils have developed O and A horizons of increasing thickness (Basdediós et al. 2022b). Soil organic matter (SOM) accumulated more rapidly, and soil development progressed faster than in other comparable young temperate alpine recession areas (Düming et al. 2011; Zimmer et al. 2024). The parent material of soil formation is a moraine consisting mainly of granitoids with admixed metamorphic rocks (Basdediós et al. 2022a). The minerals comprise mainly silicates (~90%), carbonates (< 6%) and phosphates (< 2%) (Zhou et al. 2016).

Field sampling

In September/October 2014 we conducted gross mineralization and pulse-chase experiments at five ecosystem succession stages with the ages of 2–3, 24, 44, 84, and 124 years (Figs. S1 and S2). Three years later (i.e., in 2017) we sampled soils and plant compartments of dominating tree species from six ecosystem succession stages, which were exposed for 0, 37, 47, 59, 87 and 127 years since glacial retreat (Fig. S1). To prevent any cross-contamination, samples from the same site age collected in different years were taken from separate plots within the same site age.

Soil profiles were hand-dug and five soil horizons sampled: Oi (fresh litter), Oe (shredded litter), Oa (dark layer of decomposed humus), A (surface mineral soil with humus enrichment), and C (weathered soil parent material). Each succession stage was sampled in triplicate, with a minimum distance of 20 m between soil profiles, except at the 0 yr-old site where the distance was reduced to 10 m because of the narrower valley near the glacier.

Samples of leaves/needles, branches, bark, wood and roots of the dominant tree species growing in the vicinity of our soil profiles were collected between August and October 2017, as described in Basdediós et al. (2022b). Four tree species were sampled along the chronosequence including *H. tibetana* (37 yr-old site), *P. purdomii* (47 yr-old site), *A. fabri* (59 and 87 yr-old sites) and *P. brachytyla* (127 yr-old site). At each replicate plot, a minimum of three trees were randomly sampled. Additionally, we collected leaves/needles of *P. purdomii* at the 59 yr-old site, and *A. fabri* at the 47 and 127 yr-old sites, which were the second more abundant tree species at those sites (Basdediós et al. 2022b).

Litterfall was collected weekly from August to October 2017 with three self-constructed collectors (closed polyethylene net with a mesh-width < 1 mm mounted at a wooden pale and positioned 0.5 m above the soil surface, representing a surface area

of 1 m^2) at each forested study site (i.e., ≥ 37 yr-old). Litterfall samples collected on the same date at the same study site with the three collectors were bulked, homogenized and ground.

Rainfall was sampled weekly from 14 August to 2 October 2017 with 4 Hellmann-type collectors, placed on a vegetation-free area (i.e., sites < 5 yr old), which were combined and filtered through a 0.2-µm filter. As the collectors were permanently open, the collected samples represent bulk deposition (i.e., wet deposition and the soluble fraction of coarse particulate dry deposition which can sediment into the open collectors).

Litterfall, leaf, needle, branch, bark, wood and root samples were oven-dried at 40 °C for 72 h. Mineral and organic soil samples were air-dried to constant weight. Aliquots of all samples were ground using a ball mill equipped with a zirconium oxide jar.

Gross mineralization experiment

Following the pool-dilution method of Davidson et al. (1991), $^{15}NH_4Cl$ tracer (Sigma Aldrich, 98 atom% ^{15}N, 25 µg ^{15}N per core) was injected with a syringe to six 100-cm^3 stainless steel soil cores at the five study sites of the 2014 field campaign. The cores were introduced into the 0–5 cm layer, removed, closed at the bottom with a metal lid and reburied at the original position. At the ≤ 44 yr-old sites, the cores were introduced into the mineral soil while at the > 44 yr-old sites the cores were introduced into the Oa horizon. Three cores were exhumed 15 min after tracer injection, and another three cores were exhumed 24 h later. At the ≤ 44 yr-old sites, the air temperatures ranged from 10 to 14 °C when the mineralization experiment started, while it rained. At the > 44 yr-old sites, air temperature ranged from 12 to 14 °C and there was only slight rain during the night. After sampling, the cores were immediately extracted with 0.5 M KCl by shaking them for 1 h (soil:solution ratio 1:25). We chose a low KCl concentrations to avoid interferences during the ^{15}N concentration measurements.

Pulse-chase experiment

We added 200 mg of ^{15}N as $^{15}NH_4Cl$ or 9.2 mg of ^{15}N as $K^{15}NO_3$ (Sigma Aldrich, 98 atom% ^{15}N), dissolved in 4 L deionized water, to the 4 m^2 experimental plots (at the level of the soil but on top of the ground vegetation). For each N species, the ^{15}N label addition was threefold replicated at each of the five study sites (30 plots in total). Biomass and soil samples were collected before and 1, 2, 4 and 8 days after labeling. The samples consisted of the bryophyte layer and mineral soil at the 2–3 yr-old site, and the shrub, grass/herb, Oi/Oe and mineral soil/Oa layers at the remaining sites. The shrub layer only occurred on 14 of the 24 experimental plots at the ≥ 24 yr-old sites and was sampled at a height of 10–30 cm. We were unable to sample the trees. The soil samples were immediately extracted with 0.5 M KCl. Soil moisture was determined gravimetrically on separate sample aliquots. Extracts were stored at approximately 5 °C. Plant samples were air-dried and ground with a ball mill (PM 200, Retsch, Haan, Germany). In the course of the experiment, the air temperature ranged between 6.2 and 14.4 °C during the day. The experiments on the ≤ 44 yr-old sites were conducted under wetter conditions (1 dry day) than those at the > 44 yr-old sites (5 dry days).

Our ^{15}N additions in small quantities, but in highly ^{15}N-enriched form have the advantage of exerting minimal influence on the native N pool size, both in the gross mineralization and the pulse chase experiments. Assuming N concentrations near the instrumental detection limit of 30 µg g^{-1} N, a mean bulk density of ~ 1.00 g cm^{-3}, and a topsoil thickness of 5 cm, the added tracer represented < 0.1% of the total N pool in the mineralization experiment and < 0.3% of the total N pool in the pulse-chase experiment.

Chemical analyses

The pH value of the mineral soil was determined with a glass electrode (WTW SenTix 81) in a 1:5 (v/v) soil:water suspension. To determine Mo and V concentrations, we digested the soil samples with $HNO_3/HF/H_2O_2$ (4:1.5:1) and the plant samples with HNO_3/H_2O_2 (4:1) in a microwave oven (MARS6Xpress, CEM, Kamp-Lintfort, Germany). The metal concentrations were measured with inductively-coupled plasma mass spectrometry (ICP-MS, 7900 Agilent, Waldbronn, Germany). Accuracy was assessed by the analysis of the certified reference materials BCR2 (Columbia River Basalt 2) for soil samples and SRM1515 (apple leaves) and SRM1547 (peach leaves) for organic

samples. Mean recoveries ± standard deviation were 100 ± 10% for all certified element concentrations. Precision determined by duplicate measurements was < 5%. The concentrations of NH_4^+, NO_3^- and total nitrogen (TN) in bulk deposition and the extracts of the gross mineralization and pulse-chase experiments were measured by continuous flow analysis (CFA, AutoAnalyzer 3 HR, Seal GmbH, Norderstedt, Germany or San++, Skalar, Breda, the Netherlands). We determined C concentrations with an Elemental Analyzer (Vario EL, Elementar Analysensysteme, Langenselbold, Germany).

Mineral soil samples, organic horizons (Oi, Oe and Oa), litterfall and roots, bark, branches, wood and leaves/needles of the dominant tree species growing along the chronosequence were analyzed for N concentrations and $\delta^{15}N$ values with an Elemental Analyzer-Isotope Ratio Mass Spectrometer (IRMS, Flash 2000 HT Plus/Delta V Advantage, Thermo Scientific, Bremen, Germany). Instrumental drift was corrected using bracket measurements of the certified isotopic reference material EMA-P2 (unknown compound, −1.57‰) as a working standard. For calibration, we used certified standards of $(NH_4)_2SO_4$ (USGS-25, IAEA-N-1, IAEA-N-2; certified $\delta^{15}N$ values = −30.41, 0.43 and 20.41‰, respectively), caffeine (USGS-61 and USGS-62; –2.87 and 20.17‰, respectively) and glycine (USGS-64, 1.76‰).

To determine the ^{15}N concentrations in NH_4^+, we used the diffusion method of Brooks et al. (1989) including the modifications of Aigner (2000), as described in the supplementary material (Method S1). The N isotopic composition of the labeled NH_4^+, plant and soil samples was measured with an EA-IRMS (vario EL/Isoprime 100, Elementar Analysensysteme). For calibration, we used the certified standards IAEA-NO3 (KNO_3, certified $\delta^{15}N$ value: 4.7‰), IAEA-N-2 and EMA-P2.

The N isotopic composition of NO_3^- extracted from the soils in the pulse chase experiment was determined by abiotic conversion to N_2O following the method of Lachouani et al. (2010), as described in Method S2. The N isotope ratio of the produced N_2O was measured with a trace gas-isotope ratio mass spectrometer (TG-IRMS, Trace Gas-Isoprime 100, Elementar-Analysensysteme).

Calculations

Annual total N input via bulk deposition was calculated by multiplying our TN concentrations (mg L^{-1}) by the mean precipitation records at the Hailuogou Meteorological Station (1947 L m^{-2}; 2948 m a.s.l.; Wu et al. 2013). The proportion of N derived from the atmosphere (*%Ndfa*) by biological N_2 fixation through the *H. tibetana* actinobacteria symbiosis was calculated as described by Unkovich et al. (2008; Eq. 1).

$$\%\mathrm{Ndfa} = \left[\left(\delta^{15}\mathrm{N}_{\mathrm{soil}} - \delta^{15}\mathrm{N}_{\mathrm{veg}}\right)/\left(\delta^{15}\mathrm{N}_{\mathrm{soil}} - \delta^{15}\mathrm{N}_{\mathrm{atm}}\right)\right] * 100 \quad (1)$$

where $\delta^{15}N_{soil}$ denotes the $\delta^{15}N$ value of the mineral soil, $\delta^{15}N_{veg}$ refers to the $\delta^{15}N$ value of the whole vegetation, and $\delta^{15}N_{atm}$ represents the atmospheric $\delta^{15}N$ value (0‰).

The N stocks in each soil organic layer and in the mineral horizon (up to 10 cm) were calculated considering the N concentration, the bulk density and the thickness of the respective horizon, as described in Basdediós et al. (2022b). A mixing model was applied to calculate the $\delta^{15}N$ values of the upper 10 cm of the mineral soil ($\delta^{15}N_{10cm}$), including the A and part of the C horizon (the A horizon was ≤ 6 cm thick along the chronosequence) at each site age (Eq. 2).

$$\delta^{15}\mathrm{N}_{10\mathrm{cm}} = \left(\left(\delta^{15}\mathrm{N}_{\mathrm{A}} * \chi_{\mathrm{A}}\right) + \left(\delta^{15}\mathrm{N}_{\mathrm{C}} * \chi_{\mathrm{C}}\right)\right)/\chi_{10\mathrm{cm}} \quad (2)$$

where $\delta^{15}N_A$ and $\delta^{15}N_C$ represent the N isotope compositions of the mineral A and C horizons, respectively, and χ_A and χ_C represent the contribution of each horizon to the total stock (χ_{10cm}), in g m^{-2}.

The N stocks ($N_{plant\ compartment}$) in the different tree compartments (leaves/needles, branches, trunk, bark, and roots) of the dominant shrub or tree species at each site were calculated by multiplying the corresponding compartment biomass (B_c) with the N concentrations measured in the different compartments (C_N), as described in Eq. 3. Total N stock in the vegetation ($N_{vegetation}$) was calculated by summing up all individual plant compartments.

$$\mathrm{N}_{\mathrm{plant\ compartment}}\left(\mathrm{g\ m^{-2}}\right) = \mathrm{B_c}\left(\mathrm{g\ m^{-2}}\right) * \mathrm{C_N}\left(\mathrm{g\ g^{-1}}\right) \quad (3)$$

The $\delta^{15}N$ values of the whole vegetation ($\delta^{15}N_{vegetation}$) were calculated by taking into account the contribution (χ; g m^{-2}) of each compartment (leaves/needles, branches, trunk and roots) to the total vegetation biomass ($\chi_{1+}\ \chi_{2+}\ldots$; g m^{-2}, Eq. 4).

$$\delta^{15}N_{vegetation} = \left(\delta^{15}N_1 * \chi_1 + \delta^{15}N_2 * \chi_2 + \dots\right)/\left(\chi_1 + \chi_2 + \dots\right) \quad (4)$$

The high C:N ratio in the trunk of the tree species growing at > 40 yr-old sites did not allow us to measure the $\delta^{15}N$ value precisely. Therefore, we have calculated the $\delta^{15}N_{vegetation}$ assuming a minimum $\delta^{15}N$ value of −3‰ ($\delta^{15}N_{vegetation\ min}$) and a maximum $\delta^{15}N = 12‰$ ($\delta^{15}N_{vegetation\ max}$), in line with the literature (Table S1).

To calculate gross N transformation, we used the isotope pool dilution method which assumes that there is no isotope fractionation during the transformations and that the rate of transformation is constant during the experiment (Kirkham and Bartholomew 1954; Davidson et al. 1991). These assumptions are usually valid for short experiment times of up to 24 h (Davidson et al. 1991). Gross N mineralization rates were calculated with Eq. 5.

$$r[I] = \frac{[I]t_0 - [I]t}{t} \cdot \frac{\log\left(\frac{[APE]t_0}{[APE]t}\right)}{\log\left(\frac{[I]t_0}{[I]t}\right)} \quad (5)$$

where r is the gross mineralization rate (mg kg^{-1} N), $[I]$ the concentration of NH_4^+ (mg kg^{-1}), t the time elapsed since the beginning of the experiment (days), t_0 the starting time of the tracer experiment and $[APE]$ the atom percent excess (atom% ^{15}N). The consumption rates of NH_4^+ were calculated with Eq. 6.

$$c[I] = r[I] - \frac{[I]t_0 - [I]t}{t} \quad (6)$$

where $c[I]$ is the consumption rate (mg N kg^{-1} soil day^{-1}) of ion I. The net ammonification rate was calculated as gross mineralization minus NH_4^+ consumption rates.

At the 2–3 yr-old site, we did not detect any NH_4^+ in one of the 24-h cores, so that the N transformation rates were calculated based on two (instead of three) replicates. Generally, occasionally low NH_4^+ concentrations around the detection limit of our EA-IRMS in the cores at the 2–3 to 44 yr-old sites increased the uncertainty of our measures of the transformation rates at the younger sites.

The biomass of the bryophyte layer was estimated by measuring its thickness (1.25 cm) and cover (25%) and assuming a bulk density of 0.1 g cm^{-3} (Yang et al. 2019). The biomass of the grass/herb and shrubs layers was taken from Luo et al. (2012) for the 24 yr-old site and adjusted to the other sites with the help of the measured height of the grass/herb and shrubs layer at each site determined by harvesting the whole 4 m^2 plot at the end of the experiment. Bulk densities of the mineral soils and Oa horizons were taken from Wang et al. (2020) for the same study sites. For the Oi/Oe layer we assumed a bulk density of 0.025 g cm^{-3} (Chojnacky et al. 2009). The volumetric stone content was visually estimated in the field using reference charts after excavation of the soil profile, and subtracted from the total horizon mass.

The recovery (%) of the added ^{15}N tracer in the pulse-chase experiment was calculated using Eq. 7 for the soil and Eq. 8 for the biomass compartments,

$$\text{Recovery}^{15}N_{soil} = \frac{Ex^{15}N * TN * \rho * d * (1 - s)}{^{15}N} \quad (7)$$

$$\text{Recovery}^{15}N_{biomass} = \frac{Ex^{15}N * TN * b}{^{15}N} \quad (8)$$

where $Ex^{15}N$ represents the concentration of ^{15}N after subtracting the ^{15}N prior to labeling (mg ^{15}N g^{-1} N), TN the total N concentration (g N kg^{-1}), ρ the bulk density (kg m^{-3}), d the thickness of the horizon (m), s the stone fraction, ^{15}N the total tracer added (mg ^{15}N m^{-2}), and b the biomass of grass/herb or shrub layer (kg m^{-2}).

The recovery (‰) of ^{15}N in the NO_3^- pool after amendment with $^{15}NH_4^+$ was calculated using Eq. 9:

$$\text{Recovery}^{15}N(‰) = \frac{Ex^{15}N * Npool}{\text{Total}^{15}N\text{applied}} * 1000 \quad (9)$$

where $Npool$ represents the total N concentration in the NO_3^- pool (mg m^{-2}).

Statistical analyses

One-way analysis of variance (ANOVA) and Tukey's HSD post-hoc tests were applied to detect significant differences between total N stocks and $\delta^{15}N$ values among the various study sites. Differences between the maximum and minimum calculated $\delta^{15}N$ values for vegetation were tested for significant differences using independent two-sample t-tests. Statistical analyses were conducted with the statistical software R (R Core Team 2020). Significance was set at $p < 0.05$.

Results

Along the chronosequence, the pH decreased from around 8, driven by the carbonic acid/ carbonate buffer system, to around 5, driven by the strong acid/ aluminium oxide buffer system (Table 1). Total N and organic C (C_{org}) in the mineral topsoil increased.

The mean N concentration of the organic horizons increased with increasing depth (Oa > Oe > Oi; Fig. 1A). Total N stocks tended to increase with increasing site age. The mean N accumulation rate in the organic layer (± standard error) and the uppermost 10 cm of the mineral soil, i.e., the root zone, was 4.3 ± 0.9 g m^{-2} yr^{-1} and that in the whole ecosystem was 4.5 ± 1.0 g m^{-2} yr^{-1}. The fastest N accumulation occurred between 37 and 47 years after glacial retreat, coinciding with the transition from the N_2-fixing *H. tibetana* actinobacterium symbiosis, with its larger N stock (Fig. 1B), to a *P. purdommii*-dominated forest. We estimated that 81% of the N stock at the 37 yr-old site was fixed from the atmosphere (%Ndfa, Eq. 1). After the establishment of the conifer-dominated forest, the annual N accumulation tended to decrease (Fig. 1A). The annual bulk deposition of TN was 0.9 g m^{-2} yr^{-1}.

The $\delta^{15}N$ value in the upper 10 cm of the mineral soil varied between 0.0 ± 0.4 ‰ (0 yr-old site) and 1.8 ± 0.2 ‰ (59 yr-old site) and was not correlated with site age (Fig. 2A). The thickness-weighted mean $\delta^{15}N$ values of the organic layer (Oi + Oe + Oa) ranged from -1.8 ± 0.2 to -1.0 ± 0.3 ‰ along the chronosequence and did not significantly differ among the sites (Fig. 2A). The N concentrations and $\delta^{15}N$ values of litterfall decreased from 20 ± 0.8 to 15 ± 0.7 g kg^{-1} (Table S2) and from -0.7 ± 0.2 ‰ to -3.3 ± 0.5 ‰ (Fig. 2A) between the 37 and the 127 yr-old sites, respectively. These changes paralleled a decrease in total N stocks (Fig. 1B) and in $\delta^{15}N$ values (Fig. 2B) in the vegetation with increasing site age. The $\delta^{15}N$ value of the vegetation decreased with increasing site age no matter if we assumed the minimum or the maximum $\delta^{15}N$ value of the trunk taken from the literature (Fig. 2B). Only if the $\delta^{15}N$ of the trunk of the tree species growing on the 127 yr-old site was > 35‰ there would not be a negative temporal trend. Such high $\delta^{15}N$ values have not been reported for vegetation compartments to date (Table S1). The $\delta^{15}N$ value of the whole ecosystem (i.e., the upper 10 cm of the mineral soil, the organic layer and the vegetation combined) varied between 0.0 ± 0.4 ‰ and -2.0 ± 0.5 ‰, and tended to decrease with increasing site age (Fig. 2C). Additionally, we measured N concentrations and $\delta^{15}N$ values of leaves/needles of the second most abundant tree species at each site (Fig. S3). No significant differences were found between leaves/needles of tree species of the same site age. Therefore, we present the results based solely on the contribution of the dominant tree species to the total biomass.

N transformation rates

The total concentrations of the KCl-extractable N species in the topsoil (i.e., mineral soil at sites ≤ 44 yr and Oa horizon at sites > 44 yr-old) increased with increasing site age. Generally, KCl-extractable organic N and NH_4^+ contributed significantly more than NO_3^- to the total KCl-extractable N species (Fig. S4). The gross mineralization and NH_4^+ consumption rates in the 0–5 cm soil layer paralleled each other and showed a positive relationship with ecosystem age (Fig. 3). Net NH_4^+ mineralization rates were near zero or even negative indicating net immobilization during our experiment except at the oldest site, where a small net NH_4^+ mineralization was observed.

^{15}N tracer recovery in the pulse-chase experiment

The lowest recoveries of the amended $^{15}NH_4^+$ and $^{15}NO_3^-$ were recorded at the 2–3 yr-old site (< 20% for both N species, Fig. 4A and B). The cumulative recovery increased with site age for both N species, except for a comparatively low total recovery of $^{15}NH_4^+$ at the 84 yr-old site (Fig. 4G, Table S3).

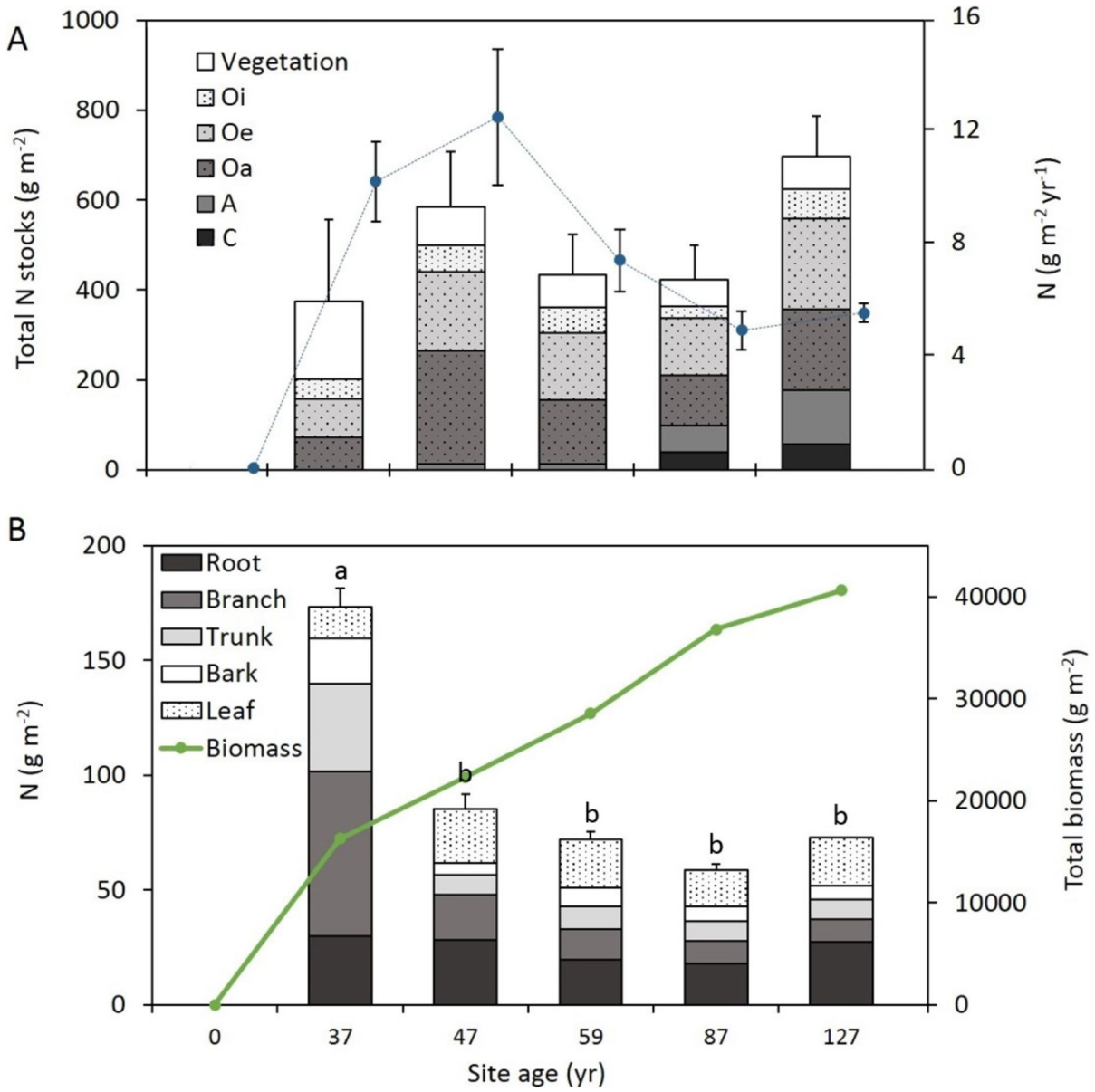

Fig. 1 Cumulative total stocks of N in the organic layer (Oa, Oe and Oi), the upper 10 cm of the mineral soil (A and C horizons) and vegetation (**A**) and cumulative N stocks in the different plant compartments of the dominant tree and shrub species (**B**) along the Hailuogou chronosequence. The blue circles and the dashed line in (**A**) represent the N accumulation rate. The green line in (**B**) represents the total biomass at our study sites based on data from Luo et al. (2004). Letters indicate significant differences according to Tukey's HSD post-hoc test. Error bars represent the standard error ($n = 3$)

At the 2–3 yr-old site, 10–15% of the amended $^{15}NH_4^+$ and 11–21% of the amended $^{15}NO_3^-$ were recovered in the bryophyte layer (Fig. 4A and B), while the tracer assimilation by the sparse vascular plant biomass played a minor role (< 4% of the amended ^{15}N). The N concentration in the mineral soil was below the instrumental detection limit (30 μg kg^{-1} N), making it impossible to determine the label's recovery in the mineral soil, which may partly explain the overall low label recovery at this site. At the 24 yr-old site, ~ 70% of both $^{15}NH_4^+$ and $^{15}NO_3^-$ were recovered on Day 1 largely because of

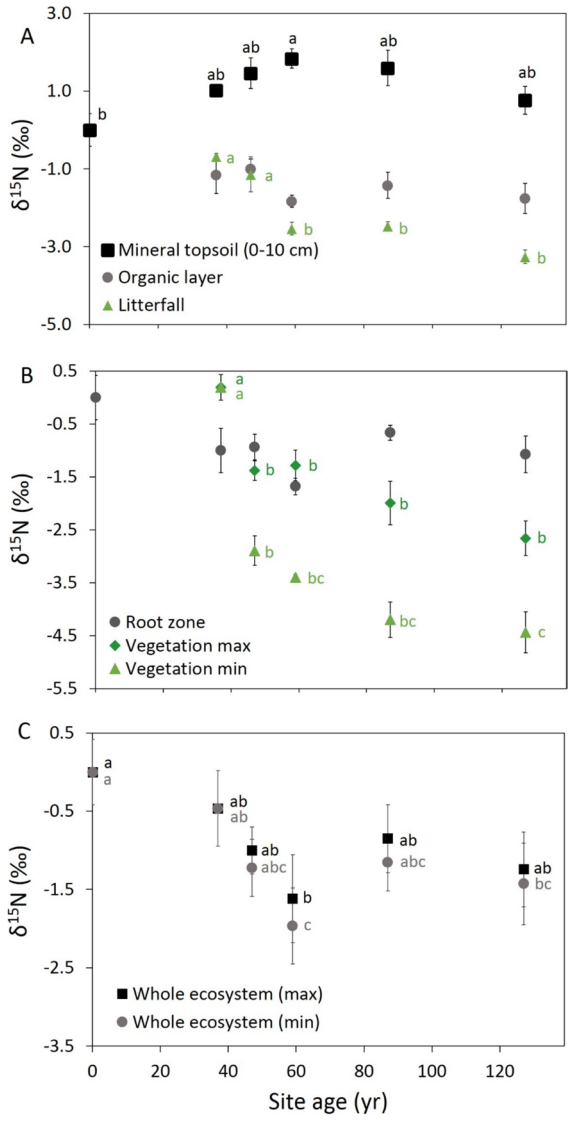

Fig. 2 Mean $\delta^{15}N$ values of the organic layer, litterfall and mineral topsoil (0–10 cm) (**A**), the root zone (organic layer + upper 10 cm of the mineral soil) and vegetation (**B**) and the whole ecosystem (**C**) along the Hailuogou chronosequence. To estimate the $\delta^{15}N$ values of the vegetation at the > 40 yr-old sites we had to assume a minimum and a maximum value for the wood from the literature resulting in a lower and upper boundary of the $\delta^{15}N$ value (min–max), because we were unable to measure the $\delta^{15}N$ values in our laboratory. The youngest ecosystem site (i.e., the 0 yr-old site) lacks both vegetation and organic layer. Letters indicate significant differences between sites according to Tukey's HSD post-hoc test. Error bars represent standard errors ($n = 3$; except for litterfall, where $n = 7$)

its accumulation in the Oi/Oe layer, while in the vascular plant and bryophyte biomass the tracer accumulated more steadily with time (Fig. 4C and D). At both the 2–3 and 24 yr-old sites, more of the $^{15}NH_4^+$ relative to $^{15}NO_3^-$ was accumulated in the biomass, while the opposite occurred in the uppermost soil layer. At the 84 yr-old site, the total recovery at the end of the experiment differed strongly between the two N species ($^{15}NH_4^+$: 18% and $^{15}NO_3^-$: 60%, Fig. 4G and H). This difference was mostly attributable to the enrichment of $^{15}NO_3^-$ in the uppermost 5 cm layer of the mineral topsoil/Oa horizon (17%) and the Oi/Oe horizons (20%), while the uppermost 5 cm layer of the mineral soil/Oa horizon (0%) and the Oi/Oe horizons (4%) played a minor role in the retention of $^{15}NH_4^+$. The cumulative recovery of both N species was highest at the 124 yr-old site (Fig. 4I and J).

^{15}N recovery in the NO_3^- pool of the soil

The recovery of the amended $^{15}NH_4^+$ in the NO_3^- pool of the uppermost 5 cm layer of the A or Oa horizons, which is indicative of nitrification, only accounted for a few permil of the added amount (< 2‰, Fig. 5). At the younger sites (< 44 yr-old), the recovery was highest on Day 1 and slightly decreased thereafter, while at the ≥ 84 yr-old sites the recovery did not change during the course of the experiment. At the end of the experiment (Day 8), the recovery was significantly higher at the 124 yr old site compared to the other sites (Fig. 5).

Discussion

Nitrogen accumulation and sources

The fact that the total N stocks in the whole ecosystem (0–10 cm layer of the mineral soil, organic layer and vegetation together) increased with site age (Fig. 1A) confirmed our first hypothesis. Nitrogen accumulated along the chronosequence at a faster rate (4.5 g N m^{-2} yr^{-1}) than at the Werenskiold glacier (1.1 g N m^{-2} yr^{-1} in the first four decades after deglaciation, Kabala and Zapart 2012) and the Glacier Bay chronosequence (2.8 g N m^{-2} yr^{-1} at the pioneer stage, where N_2-fixing species were dominant, and 0.2 g N m^{-2} yr^{-1} in the later stages; Bormann and Sidle 1990). The N accumulation rate in the Hailuogou glacial retreat area was one order of magnitude larger than the values reported for the Swiss Alps (0.3–0.5 g N m^{-2} yr^{-1}; Egli et al. 2001)

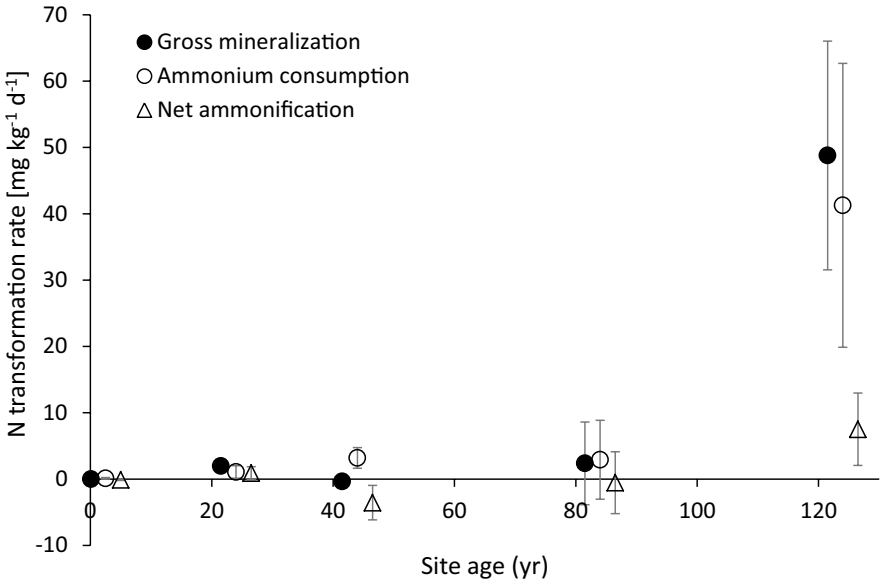

Fig. 3 Relationship between site age and gross mineralization (filled circles), NH_4^+ consumption (open circles) and net ammonification (open triangles) in the 0–5 cm soil layer (A horizon at the ≤ 44 yr-old sites, Oa horizons at the > 44 yr-old sites). Error bars show standard errors of three replicate plots (2–3 yr-old site only two replicates) and are visible if larger than the symbol. The data points were horizontally slightly shifted to increase clarity

or the Lake Michigan sand dunes (0.3 g N m^{-2} yr^{-1}; Lichter 1998).

The input of N via bulk deposition of 0.9 g m^{-2} is similar to the 0.85 g m^{-2} estimated by Liu et al. (2008) for the same study region in the year 2007 based on N concentrations in moss as indicator plant, and slightly higher than the 0.74 g m^{-2} measured by Song et al. (2017) between 2008 and 2013. The bulk deposition of 0.9 g m^{-2} is larger than in the glacier retreat areas of the Franz Josef glacier in New Zealand or Glacier Bay in Alaska (< 0.2 g m^{-2} yr^{-1}; Menge and Hedin 2009, Sullivan et al. 2011), but still slightly below the critical N load in temperate forests (1.0–1.5 g m^{-2}; Bobbink et al. 2010), which might even be exceeded if the unknown dry deposition was added. Assuming that the N input via bulk deposition has been constant since deglaciation, our youngest studied site with a full vegetation cover (i.e., the 37 yr-old site of the 2017 sampling campaign) would have received 35 g m^{-2} of N which accounts for ~ 9% of the total stock of N (380 ± 180 g m^{-2}; Fig. 1A). Following the same assumption, the oldest site would have received 119 g N m^{-2}, which accounts for ~ 17% of the total N stock (700 ± 90 g m^{-2}; Fig. 1A), suggesting that N deposition likely contributed to the rapid N accumulation, but it was not the primary source of N in the ecosystem.

Our estimation of %Ndfa indicated that the N_2-fixing *H. tibetana*-actinobacteria symbiosis at the 37 yr-old site acquired > 80% of its total N stock by N_2 fixation. This strong initial N_2 fixation was reflected by a ^{15}N value near to that of the atmospheric N (i.e., ~ 0‰) in the vegetation (Fig. 2B). Furthermore, the near-neutral pH values in the early stage of the chronosequence (Table 1), along with the likely sufficient availability of Mo and V in the parent material (2.5 ± 0.5 and 150 ± 30 mg kg^{-1} compared to the Earth's crust mean of 1.4 and 100 mg kg^{-1}, respectively; Lang 2005, Bigalke 2012), suggest favorable conditions for N_2 fixation (Robson et al. 1986), as these trace metals are key components of the three known nitrogenase enzymes that enable N_2 fixation (Bellenger et al. 2020; Reed et al. 2011). V-nitrogenases, as a complement to Mo-nitrogenases, are used by a wide range of organisms to sustain N_2 fixation under challenging environmental conditions, such as those in glacier forefields (Bellenger et al. 2020; Darnajoux et al. 2019). Although the influence of the V availability on V-nitrogenase activities remains a subject of ongoing research (Cleveland et al. 2022; Wang et al. 2023), the larger accumulation of V in the roots at the youngest vegetated site (> 40% of the total V stock in the vegetation) compared to the other vegetated sites (< 23%, Fig. S5) may indicate a greater demand for V by the plants for N_2 fixation. The particularly high N_2 fixation at the 37 yr-old site promoted the development of other non-fixing tree species such as *P. purdomii*, which took advantage of the

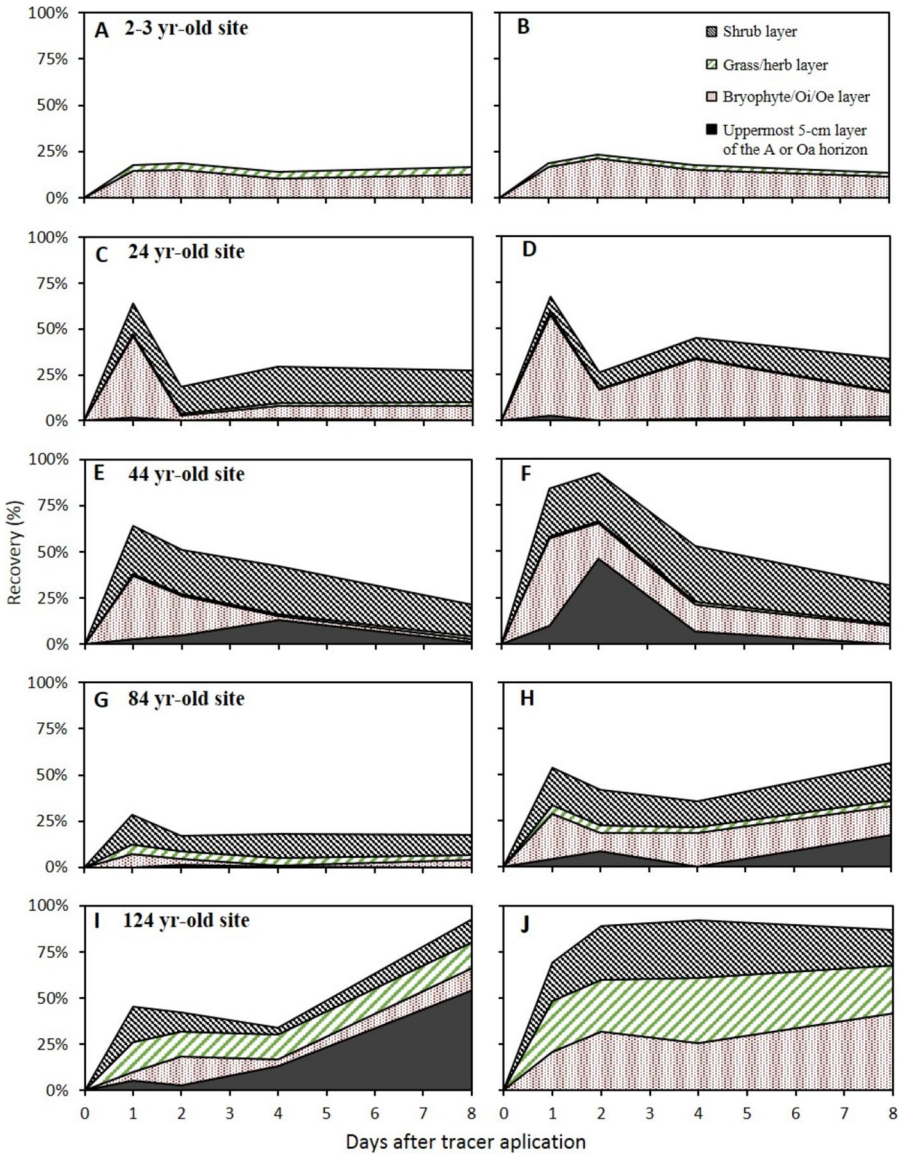

Fig. 4 Temporal course of the ^{15}N recovery in the $^{15}NH_4^+$ treatments (left column, **A**, **C**, **E**, **G**, **I**) and the $^{15}NO_3^-$ treatments (right column, **B**, **D**, **F**, **H**, **J**) along the Hailuogou chronosequence. At ≤ 44 yr-old sites, the uppermost 5-cm layer of the A horizons and at the > 44 yr-old sites of the Oa horizons were sampled. The tree layer is not included. Percentages refer to the recovery of the amended 49 mg m^{-2} $^{15}NH_4^+$ (right) and 2.25 mg m^{-2} $^{15}NO_3^-$ (left)

N-rich litterfall of *H. tibetana* to become dominant in the next succession stage (Wang et al. 2021).

With increasing site age, vegetation tended to become increasingly depleted in ^{15}N (Fig. 2B), reflected by lower $\delta^{15}N$ values and N concentrations in litterfall (Fig. 2A, Table S2). This was likely driven by a shift from deciduous to conifer-dominated forest and a microbial transition from bacteria- to fungi-dominated communities (Jiang et al. 2019), which preferentially transfer ^{14}N to the plants (Hobbie & Högberg 2012). Additionally, isotopically lighter N sources, such as bulk N deposition, may further contribute to the decreasing $\delta^{15}N$ values observed in the vegetation as site age increases (Fig. 2B).

Development of N mineralization and NH_4^+ consumption

The gross mineralization and NH_4^+ consumption rates in the soil increased with site age (Fig. 3), because of the establishment of a microbial community (Jiang et al. 2019) and increasing organic N concentrations (Fig. 1A), supporting our second hypothesis. The gross mineralization rate at the 2–3 yr-old site was lower than

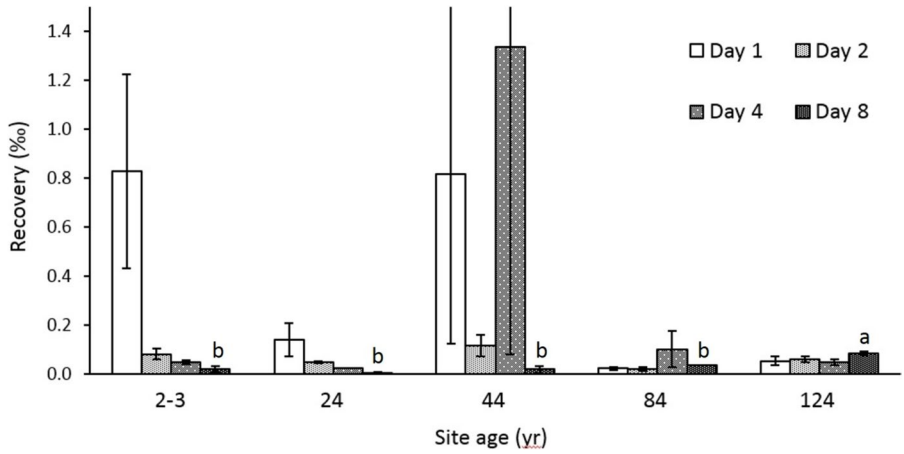

Fig. 5 ^{15}N recovery in the NO_3^- pool of the 0–5 cm layer of the soil (A horizons at ≤ 44 yr-old sites, Oa horizons at > 44 yr-old sites) after amendment of $^{15}NH_4^+$. Per mil values refer to the fraction of the amended 49 mg m^{-2} $^{15}NH_4^+$ that was found in the NO_3^- pool. Different letters indicate significant differences of the recovery on different days among sites according to Tukey's HSD post-hoc test. Error bars indicate standard errors ($n = 3$)

all values reported in Table S4, which are primarily from tropical and subtropical sites, whereas the gross mineralization rate in the Oa horizon at the 124 yr-old site was even an order of magnitude higher than most of the reported values. All other gross mineralization rates along the Hailuogou chronosequence fell within the range of data compiled in Table S4. These findings suggest that the rapid vegetation succession in the Hailuogou region is closely associated with the establishment of an intense N cycle with high transformation rates.

The NH_4^+ consumption rates were similar to the gross mineralization rates, indicating that the mineralized NH_4^+ was almost entirely taken up by microorganisms and plants, except at the 124 yr-old site (Fig. 3). Similarly to the gross mineralization rates, NH_4^+ consumption rates at the 2–3 yr-old site fell below the reported range in the literature, while those at the 124 yr-old were higher (Table S4). As a consequence, we only observed a positive net N ammonification at the oldest site, while at all other sites the net N ammonification was near to zero or even negative indicating that the microbes immobilized all available N which is typical of a strong N limitation (Fig. 3). Moreover, the low KCl-extractable NO_3^- concentration even at the ≥ 84 yr-old sites (Fig. S4D and E) indicated a consistently closed N cycle, as it suggests that available N is being efficiently taken up and used by plants and microorganisms, with minimal losses to leaching or gaseous emissions.

Because the gross mineralization, NH_4^+ consumption and net mineralization rates changed little in the first 84 years of the chronosequence, we assume that the changes of these rates between 2014 and 2017 are negligible. As consequence, a direct comparison of the N accumulation rates in Fig. 1 with the N turnover rates in Fig. 3 seems feasible.

Main ecosystem sinks of amended nitrogen

In our pulse-chase experiment, total ^{15}N retention tended to increase with increasing site age (Fig. 4), with the exception of a local decrease at the 84 yr-old site in the $^{15}NH_4^+$ treatment (Fig. 4G). Our total ecosystem recoveries at the more developed sites of the Hailuogou chronosequence (i.e., ≥ 44 yr old) were comparable to those reported for a mountain *P. abies* forest in Switzerland (50% of $^{15}NH_4^+$ and 65% of $^{15}NO_3^-$, seven days after tracer application; Providoli et al. 2006) and for an alpine grassland in northwest China (49% and 48% of $^{15}NH_4^+$ and $^{15}NO_3^-$, respectively, 14 days after tracer application; Wan et al. 2022). However, the recoveries of both ^{15}N species were lower than those reported for a boreal coniferous forest in China (91% of $^{15}NH_4^+$ and 85% of $^{15}NO_3^-$, four months after tracer application; Sheng et al. 2014). Our $^{15}NO_3^-$ recovery was comparable to that observed in a subtropical evergreen broadleaved forest in China (55%), although the $^{15}NH_4^+$ recovery

remained lower (90%; Sheng et al. 2014). Corre et al. (2010) suggested that soil type, presence of an organic layer and hydrological properties are more important drivers of N retention than the vegetation. However, at the > 44 year-old sites in the Hailuogou region, most of the amended ^{15}N was recovered in the sampled biomass (shrub and herb layers), indicating that plant uptake played an important role in retaining the ^{15}N tracer. We therefore suspect that the low total recovery of our tracer at the younger sites (i.e., ≤ 44 yr-old) was partly attributable to N leaching because of limited organismic uptake. This loss appeared to decrease progressively as the vegetation and the organic layer developed, likely because of the increased retention of N in plant biomass and soil organic matter.

At the < 84 yr-old sites, the total ecosystem recovery of ^{15}N was similar for both amended N forms, which is in line with the global patterns reported by Gurmesa et al (2022). However, after 84 years more $^{15}NO_3^-$ than $^{15}NH_4^+$ was retained in the shrub and bryophyte layers, similar to the findings of Providoli et al. (2006) for a coniferous mountain forest in Switzerland. The latter finding could be explained by a more comprehensive uptake of NO_3^- than of NH_4^+ by the vegetation of the later succession stages (Gurmesa et al. 2022), differing from the findings of Huang et al (2023b). Alternatively, it could also be attributed to the preferential immobilization of NH_4^+ by soil microbes or adsorption of NH_4^+ on the surface of soil particles and fixation in clay minerals such as illites and vermiculites (Puri and Ashman 1999; Yang et al. 2015).

At six of the ten sites, total ^{15}N recovery peaked on the first sampling date after tracer addition (Day 1, Fig. 4), which was mainly driven by uptake into the vegetation. The two cases, in which some $^{15}NO_3^-$ appeared in the mineral soil within the first two days (Fig. 4F and H) might have been influenced by NO_3^- leaching, likely because of the rainy conditions at the beginning of the experiment at the ≤ 44 yr-old sites. Overall, the results support our third hypothesis that the main N sink shifts from initial moss-dominated organism communities via the vegetation to the soil.

Transfer of amended $^{15}NH_4^+$ to the soil NO_3^- pool

The result that only a small portion of the amended $^{15}NH_4^+$ was found in the NO_3^- pool of the 0–5 cm layer of the soil (Fig. 5) indicated a low nitrification rate as a consequence of strong N limitation of the microorganism even at the oldest site (Li et al. 2020), supporting our fourth hypothesis. This conclusion was corroborated by a rough estimate of gross nitrification rates based on the $^{15}NO_3^-$ concentrations in the soil on Days 1 and 2 in the $^{15}NO_3^-$ treatment with Eq. 5 (replacing NH_4^+ by NO_3^-). The gross nitrification accounted with 2.32 mg kg^{-1} d^{-1} N only for 4.6% of the gross mineralization rate at the oldest site.

The highest recovery of ^{15}N in soil NO_3^- at the 2–3 yr-old site is attributable to the scarce plant cover of this site and associated small plant uptake (Zhou et al. 2020). With increasing duration of the experiment, the recovery of the label in the soil NO_3^- pool of the ≤ 44 yr-old sites tended to decrease, perhaps indicating a small constant left-over amount of NH_4^+, which may have contributed to the increasing microbial biomass and enzyme activities during the first 44 years (Li et al. 2020).

At the end of the experiment (Day 8) the recovery of ^{15}N in soil NO_3^- of the oldest site was significantly higher than at the other sites, suggesting that a small nitrification occurred. This was in line with the fact that this site showed a small net ammonification allowing for some nitrification (Fig. 3).

Conclusions

Our results showed that along the Hailuogou chronosequence, N accumulated at a higher rate than in other glacial retreat areas worldwide. The initial strong N_2 fixation together with the retention of deposited N facilitated the establishment of the vegetation. As the vegetation develops, the N cycle transitions into a tight internal N cycling via organic matter mineralization with little N losses. This is reflected by the near 0‰ $\delta^{15}N$ values of the whole ecosystem (vegetation, organic layer, and 0–10 cm of the mineral soil) in the early stages, which decreased during the first 60 years, stabilizing at a negative $\delta^{15}N$ value in > 60 yr-old ecosystems. We suggest that this fast change from dominant N acquisition to internal N cycling was favored by the low carbonate concentrations in the glacial debris associated with a near-neutral pH value and a sufficient Mo and V supply creating very good conditions for biological N_2 fixation at the beginning of the vegetation succession.

Gross N mineralization, NH_4^+ consumption, and net ammonification were initially low but reached

levels comparable to those of tropical forests in approximately 120 years. The maximum accumulation of deposited N shifted from the bryophyte via the shrub layer to the soil, particularly the organic layer, highlighting the important role of the organic layer for N retention. At the end of the experiment, more $^{15}NO_3^-$ tracer was recovered in older ecosystems, indicating reduced leaching losses compared to younger ones. Additionally, only a small amount of the amended $^{15}NH_4^+$ was recovered in the soil NO_3^- pool, demonstrating little nitrification, even in the oldest ecosystem despite the high gross mineralization rate indicating a tight N cycle.

Acknowledgements We thank Z. Zhong for her assistance in the field during the sampling campaign in 2017; D. Fischer for her support in the laboratory at the University of Bern; B. Bayer, T. Fabian and A. Velescu for assistance with the EA-IRMS and CFA measurements at the Karlsruhe Institute of Technology. We are indebted to the German Research Foundation (DFG, Wi 1601/25-1) and to the National Natural Science Foundation of China (NSFC, grant no. 42271064) for supporting this study. Furthermore, we thank two anonymous reviewers for their thoughtful comments on the manuscript.

Funding Open Access funding enabled and organized by Projekt DEAL.

Data availability The data that support this study will be shared upon reasonable request to the corresponding author.

Declarations

Conflicts of interest The authors have no conflicts of interest to declare.

References

Aigner M (2000) Modified micro-diffusion method for ^{15}N-enriched soil solution. IAEA-TECDOC-1164, 191–200.

Amundson R, Austin AT, Schuur EAG, Yoo K, Matzek V, Kendall C, Uebersax A, Brenner D, Bais-den WT (2003) Global patterns of the isotopic composition of soil and plant nitrogen. Global Biogeochem 17:1031. https://doi.org/10.1029/2002GB001903

Austin AT, Vitousek, PM (1998) Nutrient dynamics on a precipitation gradient in Hawai'i. Oecologia 113(4):519–529. http://www.jstor.org/stable/4221882

Basdediós N, Wu Y, Wilcke W (2022a) Base cations release in soils along the 127-year Hailuogou glacial retreat chronosequence. SSSAJ 86(6):1692–1706. https://doi.org/10.1002/saj2.2047

Basdediós N, Zhong Z, Wu Y, Wilcke W (2022b) Initial carbonate weathering is linked with vegetation development along a 127-year glacial retreat chronosequence in the subtropical high mountainous Hailuogou region (SW China). Plant Soil 471:609–628. https://doi.org/10.1007/s11104-021-05250-y

Bellenger JP, Darnajoux R, Zhang X, Kraepiel AML (2020) Biological nitrogen fixation by alternative nitrogenases in terrestrial ecosystems: a review. Biogeochemistry 149:53–73. https://doi.org/10.1007/s10533-020-00666-7

Bigalke M (2012) Vanadium. In: Litz N, Wilcke W, Wilke BM (eds): Soil-threatening substances (in German). ecomed-Verlag, Landsberg am Lech, Germany, ISBN 3–609–52000–0, since 2008 Wiley-VCH, Weinheim, Germany.

Bing H, Wu Y, Zhou J, Sun H, Luo J, Wang J, Yu D (2016) Stoichiometric variation of carbon, nitrogen, and phosphorus in soils and its implication for nutrient limitation in alpine ecosystem of Eastern Tibetan Plateau. J Soils Sediments 16:405–416. https://doi.org/10.1007/s11368-015-1200-9

Blackmer AM, Bremner JM (1977) Nitrogen isotope discrimination in denitrification of nitrate in soils. Soil Biol Biochem 9:73–77. https://doi.org/10.1016/0038-0717(77)90040-2

Blevins D (1989) An overview of nitrogen metabolism in higher plants. Plant Nitrogen Metabolism Plenum, New York, 1–41. https://doi.org/10.1007/978-1-4613-0835-5_1

Bobbink R, Hicks K, Galloway J, Spranger T, Alkemade R, Ashmore M, Bustamante M, Cinderby S, Davidson E, Dentener F, Emmett B, Erisman J-W, Fenn M, Gilliam F, Nordin A, Pardo L, De Vries W (2010) Global assessment of nitrogen deposition effects on terrestrial plant diversity: a synthesis. Ecol Appl 20:30–59. https://doi.org/10.1890/08-1140.1

Boddey RM, Peoples MB, Palmer B, Dart PJ (2000) Use of the ^{15}N natural abundance technique to quantify biological nitrogen fixation by woody perennials. Nutr Cycling Agroecosyst 57:235–270. https://doi.org/10.1023/A:1009890514844

Bormann BT, Sidle RC (1990) Changes in Productivity and Distribution of Nutrients in a Chronosequence at Glacier Bay National Park. Alaska J Ecol 78(3):561–578. https://doi.org/10.2307/2260884

Braun J, Mooshammer M, Wanek W, Prommer J, Walker TWN, Rütting T, Richter A (2018) Full ^{15}N tracer accounting to revisit major assumptions of ^{15}N isotope pool dilution approaches for gross nitrogen mineralization. Soil Biol Biochem 117:16–26. https://doi.org/10.1016/j.soilbio.2017.11.005

Brooks PD, Stark JM, McInteer BB, Preston T (1989) Diffusion method to prepare soil extracts for automated nitrogen-15 analysis. SSSAJ 53:1707–1711. https://doi.org/10.2136/sssaj1989.03615995005300060016x

Buchmann N, Gebauer G, Schulze ED (1996) Partitioning of 15N-labeled ammonium and nitrate among soil, litter, below- and above-ground biomass of trees and understory in a 15-year-old Picea abies plantation. Biogeochem 33:1–23. https://doi.org/10.1007/BF00000967

Chojnacky D, Amacher M, Gavazzi M (2009) Separating duff and litter for improved mass and carbon estimates. South J Appl for 33(1):29–34. https://doi.org/10.1093/sjaf/33.1.29

Cleveland CC, Houlton BZ, Smith WK, Marklein AR, Reed SC, Parton W, del Grosso SJ, Running SW (2013) Patterns of new versus recycled primary production in the terrestrial biosphere. PNAS 110(31):12733–12737. https://doi.org/10.1073/pnas.1302768110

Cleveland CC, Reis CRG, Perakis SS et al (2022) Exploring the Role of Cryptic Nitrogen Fixers in Terrestrial Ecosystems: A Frontier in Nitrogen Cycling Research. Ecosystems 25:1653–1669. https://doi.org/10.1007/s10021-022-00804-2

Cole DW, Rapp M (1981) Elemental cycling in forest ecosystems. Cambridge University Press, Cambridge, Dynamic Principles of Forest Ecosystems

Corre MD, Veldkamp E, Arnold J, Wright SJ (2010) Impact of elevated N input on soil N cycling and losses in old-growth lowland and montane forests in Panama. Ecology 91:1715–1729. https://www.jstor.org/stable/25680412

Craine JM, Brookshire ENJ, Cramer MD, Hasselquist NJ, Koba K, Marin-Spiotta E, Wang L (2015) Ecological interpretations of nitrogen isotope ratios of terrestrial plants and soils. Plant Soil 396(1):1–26. https://doi.org/10.1007/s11104-015-2542-1

Darnajoux R, Magain N, Renaudin M, Lutzoni F, Bellenger JP, Zhang X (2019) Molybdenum threshold for ecosystem-scale alternative vanadium nitorgenase activity in boreal forests. Proc Natl Acad Sci USA 116:24682–24688. https://doi.org/10.1073/pnas.1913314116

Davidson EA, Hart SC, Shanks CA, Firestone MK (1991) Measuring gross nitrogen mineralization, immobilization, and nitrification by 15N isotopic pool dilution in intact soil cores. J Soil Sci 42:335–349. https://doi.org/10.1111/j.1365-2389.1991.tb00413.x

Delgado-Baquerizo M, Reich PB, Bardgett RD et al (2020) The influence of soil age on ecosystem structure and function across biomes. Nat Commun 11:4721. https://doi.org/10.1038/s41467-020-18451-3

Düming A, Smittenberg R, Kögel-Knabner I (2011) Concurrent evolution of organic and mineral components during initial soil development after retreat of the Damma glacier, Switzerland. Geoderma 163:83–94. https://doi.org/10.1016/j.geoderma.2011.04.006

Egli M, Fitze P, Mirabella A (2001) Weathering and evolution of soils formed on granitic, glacial deposits: results from chronosequences of Swiss alpine environments. CATENA 45:19–47. https://doi.org/10.1016/S0341-8162(01)00138-2

Feng X, Fu B, Piao S et al (2016) Revegetation in China's Loess Plateau is approaching sustainable water resource limits. Nature Clim Change 6:1019–1022. https://doi.org/10.1038/nclimate3092

Ficetola GF, Marta S, Guerrieri A et al (2024) The development of terrestrial ecosystems emerging after glacier retreat. Nature 632:336–342. https://doi.org/10.1038/s41586-024-07778-2

Göransson H, Welc M, Bünemann EK, Christl I, Venterink HO (2016) Nitrogen and phosphorus availability at early stages of soil development in the Damma glacier forefield, Switzerland; implications for establishment of N2-fixing plants. Plant Soil 404(1–2):251–261. https://doi.org/10.1007/s11104-016-2821-5

Groffman PM, Howard G, Gold AJ, Nelson WM (1996) Microbial nitrate processing in shallow groundwater in a riparian forest. J Environ Qual 25:1309–1316. https://doi.org/10.2134/jeq1996.00472425002500060020x

Gurmesa GA, Wang A, Li S et al (2022) Retention of deposited ammonium and nitrate and its impact on the global forest carbon sink. Nat Commun 13:880. https://doi.org/10.1038/s41467-022-28345-1

Hart SC, Nason GE, Myrold DD, Perry DA (1994) Dynamics of Gross Nitrogen Transformations in an Old-Growth Forest: The Carbon Connection. Ecology 75:880–891. https://doi.org/10.2307/1939413

Hobbie EA, Hogberg P (2012) Nitrogen isotopes link mycorrhizal fungi and plants to nitrogen dynamics. New Phytol 196:367–382. https://www.jstor.org/stable/newphytologist.196.2.367

Hock R, Bliss A, Marzeion B, Giesen RH, Hirabayashi Y, Huss M, Radić V, Slangen ABA (2019) GlacierMIP – a model intercomparison of global-scale glacier mass-balance models and projections. J Glaciol 65:453–467. https://doi.org/10.1017/jog.2019.22

Hodkinson ID, Coulson SJ, Webb NR (2003) Community assembly along proglacial chronosequences in the high Arctic: vegetation and soil development in north-west Svalbard. J Ecol 91:651–663. https://doi.org/10.1046/j.1365-2745.2003.00786.x

Högberg P (1990) Forests losing large quantities of nitrogen have elevated $^{15}N/^{14}N$ ratios. Oecologia 84:229–231. https://doi.org/10.1007/BF00318276

Högberg P (1997) Tansley Review No. 95 ^{15}N natural abundance in soil–plant systems. New Phytol 137(2):179–203. https://doi.org/10.1046/j.1469-8137.1997.00808.x

Houlton BZ, Sigman DM, Schuur EA, Hedin LO (2007) A climate-driven switch in plant nitrogen acquisition within tropical forest communities. PNAS 104(21):8902–8906. https://doi.org/10.1073/pnas.0609935104

Huang Y, Shi W, Fu Q, Qiu Y, Zhao J, Li J, Lyu Q, Yang X, Xiong J, Wang W, Chang R, Yao Z, Dai Z, Qiu Y, Chen H (2023a) Soil development following glacier retreat shapes

metagenomic and metabolomic functioning associated with asynchronous C and N accumulation. Sci Total Environ 892:164405. https://doi.org/10.1016/j.scitotenv.2023.164405

Huang Y, Du L, Lei Y, Liang J (2023b) Nitrogen Preference of Dominant Species during Hailuogou Glacier Retreat Succession on the Eastern Tibetan Plateau. Plants 12(4):838. https://doi.org/10.3390/plants12040838

Hugonnet R, McNabb R, Berthier E et al (2021) Accelerated global glacier mass loss in the early twenty-first century. Nature 592:726–731. https://doi.org/10.1038/s41586-021-03436-z

IPCC (2023) Climate Change 2023: Synthesis Report. Contribution of Working Groups I, II and III to the Sixth Assessment Report of the Intergovernmental Panel on Climate Change [Core Writing Team, H. Lee and J. Romero (eds.)]. IPCC, Geneva, Switzerland, pp. 35–115. https://doi.org/10.59327/IPCC/AR6-9789291691647

IUSS Working Group WRB (2022) World Reference Base for soil resources. International soil classification system for naming soils and creating legends for soil maps. 4th edition. International Union of Soil Sciences (IUSS), Vienna. Austria. https://www.isric.org/sites/default/files/WRB_fourth_edition_2022-12-18.pdf

Jiang YL, Lei YB, Qin W, Korpelainen H, Li CY (2019) Revealing microbial processes and nutrient limitation in soil through ecoenzymatic stoichiometry and glomalin-related soil proteins in a retreating glacier forefield. Geoderma 338:313–324. https://doi.org/10.1016/j.geoderma.2018.12.023

Kabala C, Zapart J (2012) Initial soil development and carbon accumulation on moraines of the rapidly retreating Werenskiold Glacier, SW Spitsbergen, Svalbard archipelago. Geoderma 175–176:9–20. https://doi.org/10.1016/j.geoderma.2012.01.025

Khedim N, Cécillon L, Poulenard J, Barré P, Baudin F, Marta S, Rabatel A, Dentant C, Cauvy-Fraunié S, Anthelme F, Gielly L, Ambrosini R, Franzetti A, Azzoni RS, Caccianiga MS, Compostella C, Clague J, Tielidze L, Messager E, Choler P, Ficetola GF (2021) Topsoil organic matter build-up in glacier forelands around the world. Glob Change Biol 27:1662–1677. https://doi.org/10.1111/gcb.15496

Kirkham D, Bartholomew WV (1954) Equations for following nutrient transformation in soil, utilizing tracer data. Soil Sci Soc Am Proc 18:33–34. https://doi.org/10.2136/sssaj1954.03615995001800010009x

Lachouani P, Frank AH, Wanek W (2010) A suite of sensitive chemical methods to determine δ15N of ammonium, nitrate and total dissolved N in soil extracts. Rap Commun Mass Spectr 24:3615–3623. https://doi.org/10.1002/rcm.4798

Lang F (2005) Vanadium. In: Litz N, Wilcke W, Wilke BM (eds): Soil-threatening substances (in German). ecomed-Verlag, Landsberg am Lech, Germany, ISBN 3–609–52000–0, since 2008 Wiley-VCH, Weinheim, Germany.

LeBauer DS, Treseder KK (2008) Nitrogen limitation of net primary productivity in terrestrial ecosystems is globally distributed. Ecology 89:371–379. https://doi.org/10.1890/06-2057.1

Lehmann J, Lilienfein J, Rebel K, do Carmo Lima S, Wilcke W, (2004) Subsoil retention of organic and inorganic nitrogen in a Brazilian savanna Oxisol. Soil Use Manage 20:163–172. https://doi.org/10.1111/j.1475-2743.2004.tb00352.x

Li X, Xiong SF (1995) Vegetation primary succession on glacier foreland in Hailuogou. Mt Gongga Mountain Research 12(2):109–115 ((**in Chinese with English abstract**))

Li Z, He Y, Yang X, Theakstone WH, Jia W, Pu T, Liu Q, He X, Song B, Zhang N, Wang S, Du J (2010) Changes of the Hailuogou glacier, Mt. Gongga, China, against the background of climate change during the Holocene. Quat Int 218:166–175. https://doi.org/10.1016/j.quaint.2008.09.005

Li Q, Liu Y, Gu Y, Guo L, Huang Y, Zhang J, Xu Z, Tan B, Zhang L, Chen L, Xiao J, Zhu P (2020) Ecoenzymatic stoichiometry and microbial nutrient limitations in rhizosphere soil along the Hailuogou Glacier forefield chronosequence. Sci Total Environ 704:135413. https://doi.org/10.1016/j.scitotenv.2019.135413

Lichter J (1998) Rates of weathering and chemical depletion in soils across a chronosequence of Lake Michigan sand dunes. Geoderma 85:255–282. https://doi.org/10.1016/S0016-7061(98)00026-3

Lilienfein J, Wilcke W, Vilela L, Lima SdC, Thomas R, Zech W (2001) Effects of Pinus caribaea plantations on the C, N, P, and S status of Brazilian savanna Oxisols. For Ecol Manage 147:171–182. https://doi.org/10.1016/S0378-1127(00)00472-2

Liu XY, Xiao HY, Liu CQ, Li YY, Xiao HW (2008) Stable carbon and nitrogen isotopes of the moss *Haplocladium microphyllum* in an urban and a background area (SW China): The role of environmental conditions and atmospheric nitrogen deposition. Atmos Environ 42:5413–5423. https://doi.org/10.1016/j.atmosenv.2008.02.038

Luo J, Chen Y, Wu Y, Shi P, She J, Zhou P (2012) Temporal-spatial variation and controls of soil respiration in different primary succession stages on glacier forehead in Gongga Mountain. China. PLoS ONE 7(8):e42354. https://doi.org/10.1371/journal.pone.0042354

Luo J, Li W, Liao X, He Z (2004) CO2 emissions from soils of the deglaciered region on Hailuogou glacier in the past 100 years. J Mount Res 22:421–427

Mariotti A, Germon JC, Hubert P et al (1981) Experimental determination of nitrogen kinetic isotope fractionation: Some principles; illustration for the denitrification and nitrification processes. Plant Soil 62:413–430. https://doi.org/10.1007/BF02374138

Menge DN, Hedin LO (2009) Nitrogen fixation in different biogeochemical niches along a 120 000-year chronosequence in New Zealand. Ecology 90:2190–2201. https://doi.org/10.1890/08-0877.1

Perakis SS, Hedin LO (2001) Fluxes and fates of nitrogen in soil of an unpolluted old-growth temperate forest, southern Chile. Ecology 82(8):2245–2260. https://doi.org/10.2307/2680229

Providoli I, Bugmann H, Siegwolf R, Buchmann N, Schleppi P (2006) Pathways and dynamics of $^{15}NO_3^-$ and $^{15}NH_4^+$ applied in a mountain *Picea abies* forest and in a nearby meadow in central Switzerland. Soil Biol Biochem 38:1645–1657. https://doi.org/10.1016/j.soilbio.2005.11.019

Puri G, Ashman M (1999) Microbial immobilization of ^{15}N-labelled ammonium and nitrate in a temperate woodland soil. Soil Biol Biochem 31:929–931. https://doi.org/10.1016/S0038-0717(98)00172-2

R Core Team. (2020). R: A language and environment for statistical computing. R Foundation for Statistical Computing. https://www.R-project.org

Reed SC, Cleveland CC, Townsend AR (2011) Functional ecology of free-living nitrogen fixation: a contemporary perspective. Annu Rev Ecol Evol Syst 42:489–512. https://doi.org/10.1146/annurev-ecolsys-102710-145034

Robinson D (2001) δ^{15}N as an integrator of the nitrogen cycle. Trends Ecol Evol 16:153–162. https://doi.org/10.1016/S0169-5347(00)02098-X

Robson RL, Eady RR, Richardson TH, Miller RW, Hawkins M, Postgate JR (1986) The alternative nitrogenase of Azotobacter chroococcum is a vanadium enzyme. Nature 322:388–390. https://doi.org/10.1038/322388a0

Shearer G, Kohl D (1986) N2−fixation in field settings: Estimations based on natural 15-N abundance. Aust J Plant Phys 13:699–756. https://doi.org/10.1071/PP9860699

Sheng W, Yu G, Fang H, Jiang C, Yan J, Zhou M (2014) Sinks for inorganic nitrogen deposition in forest ecosystems with low and high nitrogen deposition in China. PLoS ONE 9:e89322. https://doi.org/10.1371/journal.pone.0089322

Song L, Kuang FH, Skiba U, Zhu B, Liu XJ, Levy P, Dore A, Fowler D (2017) Bulk deposition of organic and inorganic nitrogen in southwest China from 2008 to 2013. Environ Pollut 227:157–166. https://doi.org/10.1016/j.envpol.2017.04.031

Song M, Yu L, Fu S, Korpelainen H, Li C (2020) Stoichiometric flexibility and soil bacterial communities respond to nitrogen fertilization and neighbor competition at the early stage of primary succession. Biol Fertil Soils 56:1121–1135. https://doi.org/10.1007/s00374-020-01495-4

Sullivan TJ, McDonnell TC, McPherson GT, Mackey SD, Moore D (2011) Evaluation of the sensitivity of inventory and monitoring national parks to nutrient enrichment effects from atmospheric nitrogen deposition: Southeast Alaska Network (SEAN). Natural Resource Report NPS/NRPC/ARD/NRR—2011/328. National Park Service, Denver, Colorado.

Unkovich, Murray & Australian Centre for International Agricultural Research (2008) Measuring plant-associated nitrogen fixation in agricultural systems [electronic resource] / Murray Unkovich [et al.]. Australian Centre for International Agricultural Research, Canberra. https://nla.gov.au/nla.cat-vn4983827

Vitousek PM (2002) Oceanic islands as model systems for ecological studies. J Biogeogr 29:573–582. https://doi.org/10.1046/j.1365-2699.2002.00707.x

Vitousek PM, Howarth RW (1991) Nitrogen limitation on land and in the Sea: How can it Occur? Biogeochemistry 13(2):87–115. https://doi.org/10.1007/BF00002772

Vogt KA, Grier CC, Meier CE, Keyes MR (1983) Organic matter and nutrient dynamics in forest floors of young and mature Abies amabilis stands in Western Washington, as affected by fine-root input. Ecol Monogr 53:139–157. https://doi.org/10.2307/1942492

Wan Q, Yue ZW, Liu B, Liu YL, Xie MY, Li L (2022) Different fates and retention of deposited NH4+ and NO3- in an alpine grassland in northwest China: A N-15 tracer study. Environ Exp Bot 201:8. https://doi.org/10.1016/j.envexpbot.2022.104989

Wang J, Wu Y, Zhou J, Bing H, Sun H, He Q, Li J, Wilcke W (2020) Soil microbes become a major pool of biological phosphorus during the early stage of soil development with little evidence of competition for phosphorus with plants. Plant Soil 446:259–274. https://doi.org/10.1007/s11104-019-04329-x

Wang J, He Q, Wu Y, Zhu H, Sun H, Zhou J, Wang D, Li J, Bing H (2021) Effects of pioneer N_2-fixing plants on the resource status and establishment of neighboring non-N_2-fixing plants in a newly formed glacier floodplain, eastern Tibetan Plateau. Plant Soil 458:261–276. https://doi.org/10.1007/s11104-020-04462-y

Wang J, Zhao Q, Zhong Y, Ji S, Chen G, He Q, Wu Y, Bing H (2023) Biological nitrogen fixation in barren soils of a high-vanadium region: Roles of carbon and vanadium. Soil Biol Biochem 186:109163. https://doi.org/10.1016/j.soilbio.2023.109163

Wietrzyk P, Rola K, Osyczka P, Nicia P, Szymański W, Węgrzyn M (2018) The relationships between soil chemical properties and vegetation succession in the aspect of changes of distance from the glacier forehead and time elapsed after glacier retreat in the Irenebreen foreland (NW Svalbard). Plant Soil 428:195–211. https://doi.org/10.1007/s11104-018-3660-3

Wu Y, Li W, Zhou J, Cao Y (2013) Temperature and precipitation variations at two meteorological stations on eastern slope of Gongga Mountain, SW China in the past two decades. J Mt Sci 10:370–377. https://doi.org/10.1007/s11629-013-2328-y

Yan T, Fang Y, Wang J, Song H, Zhong T, Wang P (2024) Effects of long-term nitrogen addition on the shift of nitrogen cycle from open to closed along an age gradient of larch plantations in North China. Soil Biol Biochem 191:109295. https://doi.org/10.1016/j.soilbio.2023.109295

Yang Y, Wang GX, Shen HH, Yang Y, Cui HJ, Liu Q (2014) Dynamics of carbon and nitrogen accumulation and C:N stoichiometry in a deciduous broadleaf forest of deglaciated terrain in the eastern Tibetan Plateau. For Ecol Manag 312:10–18. https://doi.org/10.1016/j.foreco.2013.10.028

Yang Z, Bing H, Zhou J, Wu Y, Sun H, Luo J, Sun S, Wang J (2015) Variation of mineral composition along the soil chronosequence at the Hailuogou Glacier foreland of Gongga Mountain. Acta Pedol Sin 52:507–516. https://doi.org/10.11766/trxb201406180301

Yang X, Xu M, Zhao Y, Gao L, Wang S (2019) Moss-dominated biological soil crusts improve stability of soil organic carbon on the Loess Plateau, China. Plant Soil Environ 65:104–109. https://doi.org/10.17221/473/2018-PSE

Yang D, Luo J, Peng P, Li W, Shi W, Jia L, He Y (2021) Dynamics of nitrogen and phosphorus accumulation and their stoichiometry along a chronosequence of forest

primary succession in the Hailuogou glacier retreat area, eastern Tibetan Plateau. PLoS ONE 16(2):e0246433. https://doi.org/10.1371/journal.pone.0246433

Zhang J, Luo J, DeLuca TH, Wang G, Sun S, Sun X, Hu Z, Zhang W (2021) Biogeochemical stoichiometry of soil and plant functional groups along a primary successional gradient following glacial retreat on the eastern Tibetan Plateau. Glob Ecol Conserv 26:e01491. https://doi.org/10.1016/j.gecco.2021.e01491

Zheng M, Zhou Z, Luo Y, Zhao P, Mo J (2019) Global pattern and controls of biological nitrogen fixation under nutrient enrichment: A meta-analysis. Glob Chang Biol 25(9):3018–3030. https://doi.org/10.1111/gcb.14705

Zhou J, Wu YH, Prietzel J, Bing H, Yu D, Sun S, Luo J, Sun H (2013) Changes of soil phosphorus speciation along a 120-year soil chronosequence in the Hailuogou glacier retreat area (Gongga Mountain, SW China). Geoderma 195–196:251–259. https://doi.org/10.1016/j.geoderma.2012.12.010

Zhou J, Bing H, Wu YH, Yang Z, Wang J, Sun H, Luo J, Liang J (2016) Rapid weathering processes of a 120-year-old chronosequence in the Hailuogou glacier foreland, Mt. Gongga. SW China Geoderma 267:78–91. https://doi.org/10.1016/j.geoderma.2015.12.024

Zhou J, Zúñiga-Feest A, Lambers H (2020) In the beginning, there was only bare regolith—then some plants arrived and changed the regolith. Journal of Plant Ecology 13(5):511–516. https://doi.org/10.1093/jpe/rtaa030

Zimmer A, Beach T, Luzzadder-Beach S, Rabatel A, Encarnacion RC, Robles JL, Tarazona EJ, Temme AJAM (2024) Soil temperature and local initial conditions drive carbon and nitrogen build-up in young proglacial soils in the Tropical Andes and European Alps. CATENA 235:107645. https://doi.org/10.1016/j.catena.2023.107645